Published in final edited form as:

Mol Pharm. 2015 August 03; 12(8): 3054–3061. doi:10.1021/acs.molpharmaceut.5b00325.

Synthesis and Evaluation of ^{64}Cu-DOTA-NT-Cy5.5 as a Dual-Modality PET/Fluorescence Probe to Image Neurotensin Receptor-Positive Tumor

Huaifu Deng[†,‡], **Hui Wang**[†], **Mengzhe Wang**[†], **Zibo Li**[†], and **Zhanhong Wu**[*,†]

[†]Biomedical Research Imaging Center and Department of Radiology, University of North Carolina at Chapel Hill, Chapel Hill, North Carolina 27599, United States

[‡]PET/CT Center, The First Affiliated Hospital of Guangzhou Medical University, Guangzhou, Guangdong 510230, China

Abstract

Overexpression of neurotensin receptors (NTRs) has been suggested to play important roles in the growth and survival of a variety of tumor types. The aim of this study is to develop a dual-modality probe (^{64}Cu -DOTA-NT-Cy5.5) for imaging NTR1 expression *in vivo* with both positron emission tomography (PET) and fluorescence. In this approach, the thiol group and N terminal amino group of neurotensin analogue (Cys-NT) were chemically modified with Cy5.5 dye and DOTA chelator, respectively. After radiolabeling with ^{64}Cu, the resulting probe (^{64}Cu-DOTA-NT-Cy5.5) was evaluated in NTR1 positive HT-29 tumor model. Small animal PET quantification analysis demonstrated that the tumor uptake was 1.91 ± 0.22 and 1.79 ± 0.16%ID/g at 1 and 4 h postinjection (p.i.), respectively. The tumor-to-muscle ratio was 17.44 ± 3.25 at 4 h p.i. based on biodistribution. Receptor specificity was confirmed by the successful blocking experiment at 4 h p.i. (0.42 ± 0.05%ID/g). In parallel with PET experiment, fluorescence imaging was also performed, which demonstrated prominent tumor uptake in HT-29 model. As a proof of concept, an imaging guided surgery was performed to the fluorescent moiety of this probe and could provide potential surgery guidance for NTR positive patients. In summary, our results clearly indicated that the dual-modality probe, ^{64}Cu-DOTA-NT-Cy5.5, could serve as a promising agent to image NTR positive tumors *in vivo*.

Keywords

^{64}Cu; neurotensin; dual-modality; positron emission tomography; fluorescence imaging

Introduction

Multimodality imaging is a fast growing research area involving the integration of different imaging modalities together. As each imaging modality has its own advantages and weaknesses, the combination of two or more imaging modalities may lead to a

[*]Corresponding Author: Phone: 919-962-5254. zhanhong_wu@med.unc.edu.

Notes: The authors declare no competing financial interest.

complementary imaging approach that would not present the shortfalls of the individual modalities.[1–6] In particular, PET can provide critical *in vivo* information on the distribution of radiolabeled biomolecules with potential applications in noninvasive cancer diagnosis; and fluorescence (FL) imaging has been demonstrated to have superior sensitivity for intraoperative tumor detection (invasive surgery) when compared to conventional visual inspection.[4,7–9] Clearly, PET/FL dual modality imaging could become an attractive strategy for patient management.

The G-protein-coupled neurotensin receptor (NTR) represents a very important cancer related target, as it is overexpressed in a variety of tumors, especially prostate cancer, colorectal cancer, pancreatic cancer, breast cancer, and lung cancer.[10–13] Indeed, recent studies showed that NTRs influence the signaling on IL-8 expression and subsequent CXCR1/STAT3 signaling pathway activation in malignant tumors and induce gelsolin-mediated invasion of cancer cell through NTR1 activation.[14,15] In addition, NTR1 shows negligible or low expression in healthy tissues, which makes it a very promising specific molecular target for imaging and targeted cancer therapy.[16] Neurotensin (NT) is a tridecapeptide ligand (pGlu-Leu-Tyr-Glu-Asn-Lys-Pro-Arg-Arg-Pro-Try-Ile-Leu), which can be readily modified for pharmacokinetics optimization and for radiolabeling with various imaging isotopes. Several radio-labeled NT analogues were recently developed as a valuable tool for both imaging and therapy of NTR-positive tumors.[17–23] Our research has been focused on the NTR-targeted probes development. Previously we synthesized and evaluated the thiolated neurotensin peptide being labeled with ^{18}F-DEG-VS, which demonstrated great potential for the detection of NTR positive tumors by PET imaging.[24]

In this report, we aim to develop a NTR targeted PET/optical dual-modality imaging probe that could become an attractive agent for patient management: PET will provide critical *in vivo* information on the NTR expression *in vivo* and fluorescence imaging will facilitate intraoperative tumor detection (invasive surgery).[25] Because the Cys-NT bears both N terminal amino group and thiol functional group, fluorescent dye and radiometal chelator could be introduced to the peptide selectively. The resulting probe is further evaluated by PET and fluorescence imaging in a rodent model with NTR1-positive HT-29 tumor.

Materials and Methods

General

All chemicals and solvents were obtained from commercial sources and used without further purification. Sulfo-*N*-hydroxysulfosuccinimide (Sulfo-NHS) and ethyl-(dimethylaminopropyl) carbodiimide (EDC) were purchased from Sigma-Aldrich. 1,4,7,10-Tetraazacyclododecane-1,4,7,10-tetraacetic acid (DOTA) was obtained from Macrocyclics, Inc. Cy5.5-Mal was purchased from GE healthcare.

Synthesis of NT-Cy5.5

Thiolated Cys-NT (0.25 μmol) was dissolved in 300 μL of H_2O and added to 0.29 μmol of Cy5.5-Mal in 30 μL of dimethyl sulfoxide (DMSO) (final pH 7.0). The reaction was incubated at room temperature (RT) for 30 min. HPLC purification afforded the final

product as blue solid. The retention time of NT-Cy5.5 on analytical HPLC is 18.64 min. The product was confirmed by Q-TOF LC/MS, *m/z* is 2221.89, $C_{102}H_{143}N_{20}O_{26}S_5$; calculated $[MH]^+$, 2221.89).

Synthesis of DOTA-NT-Cy5.5

Activated DOTA (2 μmol) was prepared based on literature report. Without purification, DOTA-sNHS solution was added to NT-Cy5.5 (0.16 μmol) in 40 μL of borate buffer (pH 8.5). The reaction stayed at RT for 30 min. HPLC purification afforded the final product as blue solid after lyophilization. The retention time of DOTA-NT-Cy5.5 on analytical HPLC is 18.55 min. The product was confirmed by Q-TOF LC/MS, *m/z* is 2607.95 for $[MH]^+$, $C_{118}H_{165}N_{24}O_{33}S_5$, calculated $[MH]^+$, 2608.07).

Radiochemistry

DOTA-NT-Cy5.5 was labeled with $^{64}CuCl_2$ in ammonium acetate buffer (pH 5.5). The reaction mixture was kept at 37 °C for 60 min. Analytical HPLC was used to purify the ^{64}Cu-labeled peptide. The radioactive peak containing the desired product was collected and rotavaped to remove organic solvent. After adjusting the pH, the imaging probe was reconstituted in 1 mL 1×PBS for *in vivo* animal experiments.

In Vitro Stability

^{64}Cu-DOTA-NT-Cy5.5 was purified by HPLC. The peak containing ^{64}Cu-DOTA-NT-Cy5.5 was collected, and the solvent was removed by rotavap. The HPLC purified product was then reconstructed in PBS (1×) to 37 MBq/mL and analyzed by radio-HPLC at 30 min, 2 h, and 6 h after incubation.

Cells and Animals

The human colon adenocarcinoma cell HT-29 was obtained from the Tissue Culture Facility of UNC Lineberger Comprehensive Cancer Center. In brief, the cells were cultured in McCoy's 5A medium with 10% fetal bovine serum (FBS) in a humidified atmosphere of 5% CO_2 at 37 °C. The cells were expanded in tissue culture dishes every other day, and the medium was changed at the same time. When grown to 80% confluence, the cells were detached with 0.05% trypsin-ethylenediaminetetraacetic acid (EDTA) for cell binding assay or animal tumor injection. Animal procedures were performed according to a protocol approved by the University of North Carolina Institutional Animal Care and Use Committee. In the procedure, 4- to 6-wk-old male athymic mice (BALB/*c nu/nu*; weight, 20–30 g) were injected subcutaneously with HT-29 human colon adenocarcinoma cells at a concentration of 1×10^6 cells per 0.1 mL in the shoulder, and enough time was allowed for tumors to grow to at least 3 mm in diameter.

In Vitro Cell Binding Assay

The *in vitro* NTR1-binding affinity and specificity of DOTA-NT-Cy5.5 and Cys-NT were assessed via competitive cell binding assays using ^{125}I-NT(8-13) (Phoenix Pharmaceuticals, Inc.) as the NTR1 specific radio-ligand based on previous report.[24,26] The best-fit 50% inhibitory concentration (IC_{50}) values for HT-29 cells were calculated by fitting the data

with nonlinear regression using GraphPad Prism (GraphPad Software). Experiments were performed on triplicate samples.

Small Animal PET Imaging

Animal procedures were performed according to a protocol approved by the University of North Carolina Institutional Animal Care and Use Committee. In brief, each mouse bearing HT-29 xenograft was injected with approximately 3.7 MBq of ^{64}Cu-DOTA-NT-Cy5.5 via the tail vein (n = 3/group). The same amount of activity was injected into the blocking group with unlabeled NT (100 μg) through the tail vein. The imaging data were achieved at 1 and 4 h p.i. using a small animal PET scanner (GE eXplore Vista), with the mice under anesthesia using isoflurane (3% for induction and 2% for maintenance). The regions of interest (ROIs) were converted to counts per gram per minute based on the assumption of 1 g/mL tissue density. Dividing counts per gram per minute by injected dose gave the image ROI-derived percentage injected dose per gram tissue (%ID/g) values.

Biodistributions were performed in nude mice bearing HT-29 tumor. Animals were sacrificed under inhalation anesthesia at 4 h postinjection of 3.7 MBq of ^{64}Cu-DOTA-NT-Cy5.5. Tissues and organs of interest were excised and weighed. Radioactivity in each excised specimen was measured using a γ-counter (PerkinElmer). The mean uptake (%ID/g) was calculated for each group of animals.

In Vivo and *ex Vivo* Near-Infrared Fluorescence Imaging

In vivo fluorescence imaging was performed using the FMT 2500 imaging system (VisEn, Inc.) and analyzed using the IVIS Living Imaging 3.0 software (Caliper Life Sciences, Alameda, CA, USA). A Cy5.5 filter set was used for acquiring the fluorescence of Cy5.5 dye conjugated to DOTA-NT peptide. Identical illumination settings (lamp voltage, filters, f/stop, field of views, binning) were used for acquiring all images. Fluorescence emission images were normalized and reported as photons per second per centimeter squared per steradian (p/s/cm^2/sr). The mice received 1.5 nmol of ^{64}Cu-DOTA-NT-Cy5.5 peptide intravenously and subjected to optical imaging at 1 and 4 h p.i. For blocking studies, the probe was coinjected into mice with 100 μg of NT peptide. The tumors, tissues, and organs were dissected and subjected to ex vivo fluorescence imaging at 4 h p.i. All fluorescence images were acquired using 1 s exposure time (f/stop = 4). The mean fluorescence for each sample was reported.

Immunohistochemistry and Microscopy

The DOTA-NT-Cy5.5 was injected intravenously into HT-29 mouse model without and with a blocking dose of NT peptide. Tumors were isolated at 4 h p.i. and embedded with Paraffin, which were then sectioned in 6 μm thickness using cryostat at −25 °C and fixed in ice-cold acetone for 15 min. After washing with PBS, endogenous peroxidase was neutralized by methanol solution containing 3% (v/v) H_2O_2. The section was washed and blocked with 10% normal horse serum (Vector Laboratories, Inc.) for 1 h at RT. Vasculature was stained using CD31 antibody (Santa Cruz Biotechnology). After washing three times with PBS, detection of CD31 primary antibody was performed using a 1:200 dilution of mouse FITF-labeled secondary antibody (Vector Laboratories, Burlingame, CA). The samples were

washed with PBS three times, and then stained with 2 μg/mL of 4,6-diamidino-2-phenylindole (DAPI) for 20 min at 37 °C. Each slide was occluded with 50% glycerin buffer and was observed using a confocal laser scanning microscope (Olympus, Tokyo, Japan) equipped with a 40× objective lens.

Data Analysis

Quantitative data are expressed as mean ± SD. Means were compared using one-way ANOVA and Student's *t* test. *P* values of less than 0.05 were considered to be statistically significant.

Results

Chemistry and Radiochemistry

The synthesis of DOTA-NT-Cy5.5 is shown in Scheme 1. In the first step, NT was conjugated with Cy5.5-Mal to afford NT-Cy5.5 in 90% yield after HPLC purification. In the second step, the free carboxyl group on DOTA was activated with EDC/Sulfo-NHS and then reacted with NT-Cy5.5 at pH 8.5. The DOTA-NT-Cy5.5 was labeled with ^{64}Cu efficiently in 0.1 M NH_4OAc buffer within 60 min at 37 °C. The specific activity of ^{64}Cu-DOTA-NT-Cy5.5 was about 10.2 GBq/μmol. The radiochemical purity of ^{64}Cu-DOTA-NT-Cy5.5 was greater than 98.9%, 96.9%, and 90.8% at 30 min, 2 h, and 6 h after incubation in phosphate-buffered saline, respectively (Figure 1).

In Vitro Cell-Binding Affinity

The receptor-binding affinity of DOTA-NT-Cy5.5 was compared with that of Cys-NT using a competitive cell-binding assay (Figure 2). Both peptides inhibited the binding of ^{125}I-NT(8–13) to NTR1-positive HT-29 cells in a dose-dependent manner. The IC_{50} (the half maximal inhibitory concentration) value for DOTA-NT-Cy5.5 (0.65 ± 0.35 nmol/L) was comparable to that of Cys-NT (0.43 ± 0.15 nmol/L). The results clearly demonstrated that the modification has minimal effect on NTR binding affinity of DOTA-NT-Cy5.5.

Biodistribution and Small Animal PET Imaging

The *in vivo* tumor-targeting property of ^{64}Cu-DOTA-NT-Cy5.5 was evaluated in HT-29 xenografts (NTR1-positive) at 1 and 4 h p.i. with static PET scans. As shown in Figure 3A, the HT-29 tumors were clearly visualized with high tumor-to-background contrast. ROI analysis on PET images shows that the tumor uptake was 1.91 ± 0.22 and 1.79 ± 0.16%ID/g at 1 and 4 h p.i., respectively (Figure 3C). The NTR1-targeting specificity of ^{64}Cu-DOTA-NT-Cy5.5 was further confirmed by the effective blocking of HT-29 tumor uptake in the presence of 100 μg of unlabeled NT peptide (Figure 3B). For example, the tumor uptake was decreased from 1.79 ± 0.16%ID/g to 0.42 ± 0.05% ID/g (blocked) at 4 h p.i. ($P < 0.05$). There was no significant difference in most of the normal organs (e.g., liver, kidneys, and muscle) between these two groups. As shown in Figure 4, in order to confirm PET result, biodistribution was also performed. The biodistribution result was consistent with the PET images. The kidney had the highest uptake of ^{64}Cu-DOTA-NT-Cy5.5 with 14.24 ± 1.33%ID/g, next to the liver with 4.63 ± 0.74%ID/g at 4 h p.i. The muscle, lung, and heart

had relatively low uptake of ^{64}Cu-DOTA-NT-Cy5.5 (Figure 4). The tumor-to-muscle ratio was 17.44 ± 3.25 at 4 h p.i.

Fluorescent Imaging

The optical imaging ability of ^{64}Cu-DOTA-NT-Cy5.5 was evaluated with the fluorescence imaging system immediately after each PET scan. Similar to PET images, the HT-29 tumor lit up at all the time points examined (Figure 3D). *Ex vivo* images of ^{64}Cu-DOTA-NT-Cy5.5 were used to confirm the *in vivo* fluorescence imaging data (4 h p.i.). As shown in Figure 5, both PET and fluorescence gave good tumor to muscle contrast. The tumor, liver, and kidneys are three motifs that showed high probe uptake. Brain and other major organs have comparable background signal due to autofluorescence. Overall, the biodistribution profiles of fluorescent imaging showed similar patterns with those of PET. It worth pointing out we do observe discrepancy on tumor to liver ratio between PET and optical imaging. Based on PET imaging and biodistribution, HT-29 tumor has lower uptake than liver. However, optical imaging showed higher tumor uptake than liver. Whether this phenomena is caused by the blood in liver or the stability of the tracer needs to be further investigated in follow up studies.

Image-Guided Surgery

BALB/c nude mice with HT-29 were imaged by fluorescence imaging at 4 h postinjection of radiolabeled ^{64}Cu-DOTA-NT-Cy5.5. After preoperative evaluation of tumor lesions by PET, image-guided surgery of the tumor lesions was performed. First, the exact tumor location was identified by fluorescence imaging. Subsequently, these tumor lesions were resected, and fluorescence imaging was repeated to ensure complete resection of the tumor. In Figure 6, the feasibility of using the probe for intraoperative image-guided surgical resection of the tumor nodules is shown.

Immunohistochemistry and Microscopy

Representative images of HT-29 xenograft tumor sections isolated from animals after injection of DOTA-NT-Cy5.5 with and without a blocking dose of NT peptide are shown in Figure 7. Analysis of tumors from blocking animals showed very weak fluorescent signals compared to DOTA-NT-Cy5.5. The results clearly demonstrated the specific binding of DOTA-NT-Cy5.5 in HT-29 tumor using FL microscope (tumor localization was clearly inhibited by coinjected Cys-NT peptide).

Discussion

Molecular imaging is an emerging technology that can visualize the interactions between molecular probes and biological targets. In recent years, tremendous progress has been made to develop novel molecular imaging probes and techniques to characterize mechanisms involved in a pathologic process. Among the technologies, PET is a powerful molecular imaging technique that is used to study and visualize the metabolism, receptor/enzyme function, and biochemical mechanisms *in vivo*.[27] Fluorescence imaging with fluorophores conjugated to tumor-targeting agents can provide sensitive intraoperative detection as a visual guide, despite its *in vivo* application by the light penetration. In recent years, the

combination of fluorescence and PET imaging is rapidly emerging as a new sensitive molecular imaging technology, which could provide an attractive strategy for tumor patient management.[28–30] With this dual-modality approach, the tumor could be assessed preoperatively, with subsequent intraoperative guidance for surgical removal of the tumor lesions based on the fluorescent component of the dual-label agent.[29,31,32] In oncology, molecular imaging is mainly dependent on the availability of a specific target on tumor cells or within the tumor stroma or vasculature, and the quality of the designed labeled probe, which depends on its biodistribution, metabolism, affinity, and specificity for the target. Among the targets, NTR1 is one of the very promising targeting receptors. Accumulating evidence suggests that NTR1 play key roles in cancer growth and survival.[16,33,34] NT, a tridecapeptide ligand for NTR, acts as a mediator in tumor progression and is metabolized rapidly in plasma by endogenous peptidases. Several NT analogues have been developed and radiolabeled as a valuable tool for both imaging and therapy of NTR-positive tumors.[17–22,24,35] Although some encouraging results have been achieved in these initial studies, to our best knowledge, there is no report on peptide based NTR1 targeted multimodality imaging agent.

In this study, we developed a dual-modality PET and fluorescent imaging probe, ^{64}Cu-DOTA-NT-Cy5.5, which has been well established to have high NTR1 expression, and evaluated it in HT-29 tumor-bearing mice.[36] Because the chemical modification of a peptide could also significantly decrease receptor binding affinity, an *in vitro* cell-binding assay of DOTA-NT-Cy5.5 and NT was performed. The binding affinities of DOTA-NT-Cy5.5 and NT were not significantly different (Figure 2), as supported by the similar IC_{50} values.

The probe has good stability *in vitro*, with the radiochemical purity of more than 98.9%, 96.9%, and 90.8% at 30 min, 2 h, and 6 h after incubation in phosphate-buffered saline, respectively. Despite the reasonable *in vitro* stability, further improvement on the stability of NT analogues (especially *in vivo* stability) is warranted in future follow-up studies. Both PET and fluorescent images showed high and specific accumulation of the dual-labeled Cys-NT in the NTR1 expressing tumor lesions. The high and specific accumulation of ^{64}Cu-DOTA-NT-Cy5.5 in the NTR1-expressing tumor lesions was confirmed by blocking experiments (Figures 3, 5, and 7). In the blocking experiment, nonradioactive Cys-NT peptide significantly ($P < 0.05$) inhibited the tumor uptake of ^{64}Cu-DOTA-NT-Cy5.5 (Figures 3 and 5) at all time points, clearly demonstrating the receptor specificity of this imaging agent.

We also performed a biodistribution study to determine the uptake in liver, kidney, small intestine, spleen, heart, and other organs or tissues more accurately. As shown in Figure 4, the uptake in these organs was correlating well with that in PET imaging (Figure 3). ^{64}Cu-DOTA-NT-Cy5.5 could be cleared through renal pathway, which also leads to predominant accumulation in the kidneys. The liver also has high uptake of ^{64}Cu-DOTA-NT-Cy5.5, which is different from our previous study.[24] It is possible that the probe becomes more hydrophobic after introducing the Cy5.5 dye, which makes it also be cleared by the liver. A high tumor-to-muscle ratio (17.44 ± 3.25) was obtained at 4 h p.i., calculated by biodistribution study, which indicates that ^{64}Cu-DOTA-NT-Cy5.5 is a promising dual-modality PET tracer for imaging of NTR-1 expressing tumors. Although high binding

affinity was observed *in vitro* (IC_{50} value of 0.65 ± 0.35 nmol/L), the NTR targeted PET agent demonstrated moderate HT-29 tumor uptake *in vivo* (1.91 ± 0.22 and 1.79 ± 0.16%ID/g at 1 and 4 h p.i., respectively). The tumor uptake was determined not only by probe's target binding affinity but also by many other factors including circulation time, water solubility, stability, etc. Clearly, systematic investigation is needed to further improve the absolute tumor take in follow-up studies.

As shown in Figure 3, the tumor could be clearly located by PET scans and optical imaging, and the biodistribution pattern is consistent between these two imaging modalities except liver. Liver showed higher uptake in PET images than fluorescence images. There are two possible reasons: (1) Liver is a relatively large organ and rich of blood. Due to the limited tissue penetration capability of fluorescence signal and high absorption of blood, the liver uptake may be underestimated on optical imaging. (2) ^{64}Cu-DOTA-NT-Cy5.5 may release free ^{64}Cu *in vivo*, which could cause the higher liver uptake in PET images. In our study, we have observed good probe stability in PBS up to 6 h postincubation, which lessens the stability concern to some extent. However, additional investigation is needed before a conclusion is drawn.

In order to demonstrate the advantage of introducing fluorescence into our probe, a proof of principle imaging guided surgery is performed. The tumor was successfully identified using fluorescent imaging and removed under the fluorescence imaging guidance (Figure 6). The accumulation of the probe could also be observed using fluorescent microscope (Figure 7). Blocking experiment successfully reduced the localization of ^{64}Cu-DOTA-NT-Cy5.5 within tumor region due to the presence of excess amount of cold NT analogues. Comparable CD31 staining was observed in both groups. This preliminary study clearly demonstrates that pre- and intra-operative detection of NTR1-expressing lesions might be feasible with the newly developed PET/optical dual-modality imaging.

Conclusion

By chemical modification of Cys-NT peptide with Cy5.5 dye and DOTA chelator, we have successfully synthesized and evaluated a novel dual-modality PET/fluorescence imaging probe, ^{64}Cu-DOTA-NT-Cy5.5, as a NTR1-targeted imaging agent. Both PET and fluorescence images clearly showed specific tumor uptake and good tumor-to-background contrast. Overall, good concordance was observed between the two imaging modalities except liver. This PET/optical tumor-targeting probe not only allows the detection of NTR-1 expressing tumors by PET imaging but also integrates PET with image-guided surgery.

Acknowledgments

The authors thank Dr. John Shively for providing Cys-NT. This work was supported by the P30-CA016086-35-37 (NCI), the American Cancer Society (12199ss1-MRSG-12-034-01-CCE), NC TraCS (2KR631408), UNC Chapel Hill Department of Radiology and BRIC, and Chinese National Natural Science Foundation (No. 81201695).

References

1. Cheon J, Lee JH. Synergistically integrated nanoparticles as multimodal probes for nanobiotechnology. Acc Chem Res. 2008; 41:1630–40. [PubMed: 18698851]

2. Zhang Y, Yang Y, Cai W. Multimodality Imaging of Integrin $\alpha_v\beta_3$ Expression. Theranostics. 2011; 1:135–48. [PubMed: 21547156]
3. Nahrendorf M, Keliher E, Marinelli B, Waterman P, Feruglio PF, Fexon L, Pivovarov M, Swirski FK, Pittet MJ, Vinegoni C, Weissleder R. Hybrid PET-optical imaging using targeted probes. Proc Natl Acad Sci U S A. 2010; 107:7910–5. [PubMed: 20385821]
4. Chen K, Li ZB, Wang H, Cai W, Chen X. Dual-modality optical and positron emission tomography imaging of vascular endothelial growth factor receptor on tumor vasculature using quantum dots. Eur J Nucl Med Mol Imaging. 2008; 35:2235–44. [PubMed: 18566815]
5. Cherry SR. Multimodality imaging: beyond PET/CT and SPECT/CT. Semin Nucl Med. 2009; 39:348–53. [PubMed: 19646559]
6. Zaidi H, Prasad R. Advances in multimodality molecular imaging. J Med Phys. 2009; 34:122–8. [PubMed: 20098557]
7. Jennings LE, Long NJ. 'Two is better than one'–probes for dual-modality molecular imaging. Chem Commun. 2009; 28:3511–24.
8. Liu S, Lin TP, Li D, Leamer L, Shan H, Li Z, Gabbai FP, Conti PS. Lewis acid-assisted isotopic ^{18}F-^{19}F exchange in BODIPY dyes: facile generation of positron emission tomography/fluorescence dual modality agents for tumor imaging. Theranostics. 2013; 3:181–9. [PubMed: 23471211]
9. Seibold U, Wangler B, Schirrmacher R, Wangler C. Bimodal imaging probes for combined PET and OI: recent developments and future directions for hybrid agent development. BioMed Res Int. 2014; 2014:153741. [PubMed: 24822177]
10. Morgat C, Mishra AK, Varshney R, Allard M, Fernandez P, Hindie E. Targeting neuropeptide receptors for cancer imaging and therapy: perspectives with bombesin, neurotensin, and neuropeptide-Y receptors. J Nucl Med. 2014; 55:1650–7. [PubMed: 25189338]
11. Valerie NC, Casarez EV, Dasilva JO, Dunlap-Brown ME, Parsons SJ, Amorino GP, Dziegielewski J. Inhibition of neurotensin receptor 1 selectively sensitizes prostate cancer to ionizing radiation. Cancer Res. 2011; 71:6817–26. [PubMed: 21903767]
12. Souaze F, Dupouy S, Viardot-Foucault V, Bruyneel E, Attoub S, Gespach C, Gompel A, Forgez P. Expression of neurotensin and NT1 receptor in human breast cancer: a potential role in tumor progression. Cancer Res. 2006; 66:6243–9. [PubMed: 16778199]
13. Alifano M, Souaze F, Dupouy S, Camilleri-Broet S, Younes M, Ahmed-Zaid SM, Takahashi T, Cancellieri A, Damiani S, Boaron M, Broet P, Miller LD, Gespach C, Regnard JF, Forgez P. Neurotensin receptor 1 determines the outcome of non-small cell lung cancer. Clin Cancer Res. 2010; 16:4401–10. [PubMed: 20810387]
14. Zhou J, Yi L, Ouyang Q, Xu L, Cui H, Xu M. Neurotensin signaling regulates stem-like traits of glioblastoma stem cells through activation of IL-8/CXCR1/STAT3 pathway. Cell Signalling. 2014; 26:2896–902. [PubMed: 25200966]
15. Hashimoto K, Kyoda Y, Tanaka T, Maeda T, Kobayashi K, Uchida K, Kitamura H, Hirata K, Tsukamoto T, Masumori N. The potential of neurotensin secreted from neuroendocrine tumor cells to promote gelsolin-mediated invasiveness of prostate adeno-carcinoma cells. Lab Invest. 2015; 95:283–95. [PubMed: 25581609]
16. Dupouy S, Mourra N, Doan VK, Gompel A, Alifano M, Forgez P. The potential use of the neurotensin high affinity receptor 1 as a biomarker for cancer progression and as a component of personalized medicine in selective cancers. Biochimie. 2011; 93:1369–78. [PubMed: 21605619]
17. Bergmann R, Scheunemann M, Heichert C, Mading P, Wittrisch H, Kretzschmar M, Rodig H, Tourwe D, Iterbeke K, Chavatte K, Zips D, Reubi JC, Johannsen B. Biodistribution and catabolism of ^{18}F-labeled neurotensin(8–13) analogs. Nucl Med Biol. 2002; 29:61–72. [PubMed: 11786277]
18. Teodoro R, Faintuch BL, Nunez EG, Queiroz RG. Neurotensin(8–13) analogue: radiolabeling and biological evaluation using different chelators. Nucl Med Biol. 2011; 38:113–20. [PubMed: 21220134]
19. Buchegger F, Bonvin F, Kosinski M, Schaffland AO, Prior J, Reubi JC, Blauenstein P, Tourwe D, Garcia Garayoa E, Bischof Delaloye A. Radiolabeled neurotensin analog, ^{99m}Tc-NT-XI, evaluated in ductal pancreatic adenocarcinoma patients. J Nucl Med. 2003; 44:1649–54. [PubMed: 14530481]

20. Zhang K, An R, Gao Z, Zhang Y, Aruva MR. Radionuclide imaging of small-cell lung cancer (SCLC) using ^{99m}Tc-labeled neurotensin peptide 8–13. Nucl Med Biol. 2006; 33:505–12. [PubMed: 16720242]
21. Garcia-Garayoa E, Blauenstein P, Blanc A, Maes V, Tourwe D, Schubiger PA. A stable neurotensin-based radio-pharmaceutical for targeted imaging and therapy of neurotensin receptor-positive tumours. Eur J Nucl Med Mol Imaging. 2009; 36:37–47. [PubMed: 18690434]
22. de Visser M, Janssen PJ, Srinivasan A, Reubi JC, Waser B, Erion JL, Schmidt MA, Krenning EP, de Jong M. Stabilised ^{111}In-labelled DTPA- and DOTA-conjugated neurotensin analogues for imaging and therapy of exocrine pancreatic cancer. Eur J Nucl Med Mol Imaging. 2003; 30:1134–9. [PubMed: 12768332]
23. Sparr C, Purkayastha N, Yoshinari T, Seebach D, Maschauer S, Prante O, Hubner H, Gmeiner P, Kolesinska B, Cescato R, Waser B, Reubi JC. Syntheses, receptor bindings, in vitro and in vivo stabilities and biodistributions of DOTA-neurotensin(8–13) derivatives containing beta-amino acid residues - a lesson about the importance of animal experiments. Chem Biodiversity. 2013; 10:2101–21.
24. Wu Z, Li L, Liu S, Yakushijin F, Yakushijin K, Horne D, Conti PS, Li Z, Kandeel F, Shively JE. Facile Preparation of a Thiol-Reactive ^{18}F-Labeling Agent and Synthesis of ^{18}F-DEG-VS-NT for PET Imaging of a Neurotensin Receptor-Positive Tumor. J Nucl Med. 2014; 55:1178–1184. [PubMed: 24854793]
25. Stummer W, Pichlmeier U, Meinel T, Wiestler OD, Zanella F, Reulen HJ. Fluorescence-guided surgery with 5-aminolevulinic acid for resection of malignant glioma: a randomised controlled multicentre phase III trial. Lancet Oncol. 2006; 7:392–401. [PubMed: 16648043]
26. Alshoukr F, Prignon A, Brans L, Jallane A, Mendes S, Talbot JN, Tourwe D, Barbet J, Gruaz-Guyon A. Novel DOTA-neurotensin analogues for ^{111}In scintigraphy and ^{68}Ga PET imaging of neurotensin receptor-positive tumors. Bioconjugate Chem. 2011; 22:1374–85.
27. Phelps ME. Positron emission tomography provides molecular imaging of biological processes. Proc Natl Acad Sci U S A. 2000; 97:9226–33. [PubMed: 10922074]
28. Vahrmeijer AL, Hutteman M, van der Vorst JR, van de Velde CJ, Frangioni JV. Image-guided cancer surgery using near-infrared fluorescence. Nat Rev Clin Oncol. 2013; 10:507–18. [PubMed: 23881033]
29. Liu S, Li D, Huang CW, Yap LP, Park R, Shan H, Li Z, Conti PS. Efficient construction of PET/fluorescence probe based on sarcophagine cage: an opportunity to integrate diagnosis with treatment. Mol Imaging Biol. 2012; 14:718–24. [PubMed: 22476968]
30. Ocak M, Gillman AG, Bresee J, Zhang L, Vlad AM, Muller C, Schibli R, Edwards WB, Anderson CJ, Gach HM. Folate receptor-targeted multimodality imaging of ovarian cancer in a novel syngeneic mouse model. Mol Pharmaceutics. 2015; 12:542–53.
31. Huang M, Xiong C, Lu W, Zhang R, Zhou M, Huang Q, Weinberg J, Li C. Dual-modality micro-positron emission tomography/computed tomography and near-infrared fluorescence imaging of EphB4 in orthotopic glioblastoma xenograft models. Mol Imaging Biol. 2014; 16:74–84. [PubMed: 23918654]
32. Muselaers CH, Rijpkema M, Bos DL, Langenhuijsen JF, Oyen WJ, Mulders PF, Oosterwijk E, Boerman OC. Radionuclide and fluorescence imaging of clear cell renal cell carcinoma using dual-labeled anti-Carbonic Anhydrase IX antibody G250. J Urol. 2015; 194:532–538. [PubMed: 25686542]
33. Vincent JP, Mazella J, Kitabgi P. Neurotensin and neurotensin receptors. Trends Pharmacol Sci. 1999; 20:302–9. [PubMed: 10390649]
34. Moody TW, Chan D, Fahrenkrug J, Jensen RT. Neuropeptides as autocrine growth factors in cancer cells. Curr Pharm Des. 2003; 9:495–509. [PubMed: 12570813]
35. Maschauer S, Greff C, Einsiedel J, Ott J, Tripal P, Hubner H, Gmeiner P, Prante O. Improved radiosynthesis and preliminary in vivo evaluation of a F-labeled glycopeptide-peptoid hybrid for PET imaging of neurotensin receptor 2. Bioorg Med Chem. 2015; 23:4026. [PubMed: 25691211]
36. Myers RM, Shearman JW, Kitching MO, Ramos-Montoya A, Neal DE, Ley SV. Cancer, chemistry, and the cell: molecules that interact with the neurotensin receptors. ACS Chem Biol. 2009; 4:503–25. [PubMed: 19462983]

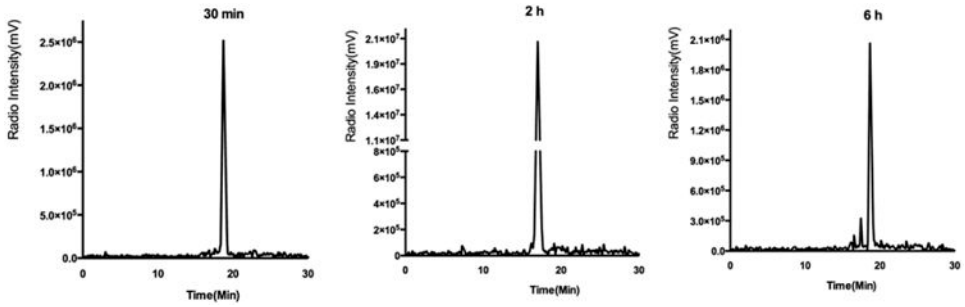

Figure 1.

HPLC profiles of ^{64}Cu-DOTA-NT-Cy5.5 at 30 min, 2 h, and 6 h after purification with radiochemical purity more than 98.9%, 96.9%, and 90.8%, respectively.

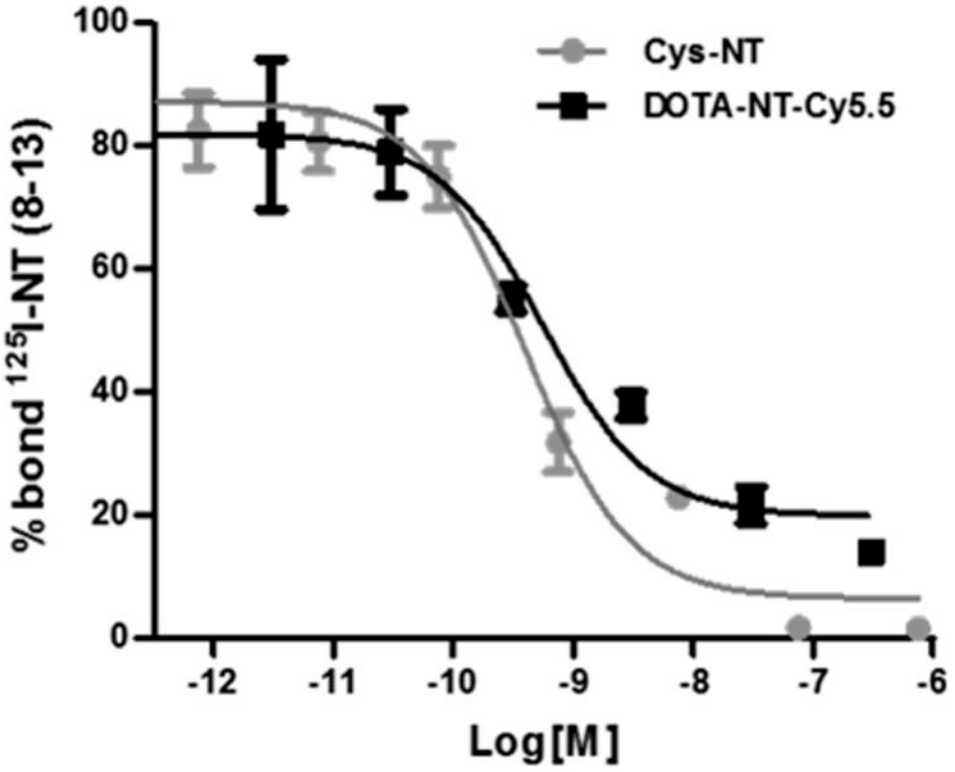

Figure 2.

Competitive cell binding assays of ^{125}I-NT(8–13) and DOTA-NT-Cy5.5 or Cys-NT in HT-29 cells. *X*-axis stands for the concentration of nonradiolabeled competitor. IC_{50} values for DOTA-NT-Cy5.5 and Cys-NT were 0.65 ± 0.35 and 0.43 ± 0.15 nmol/L, respectively.

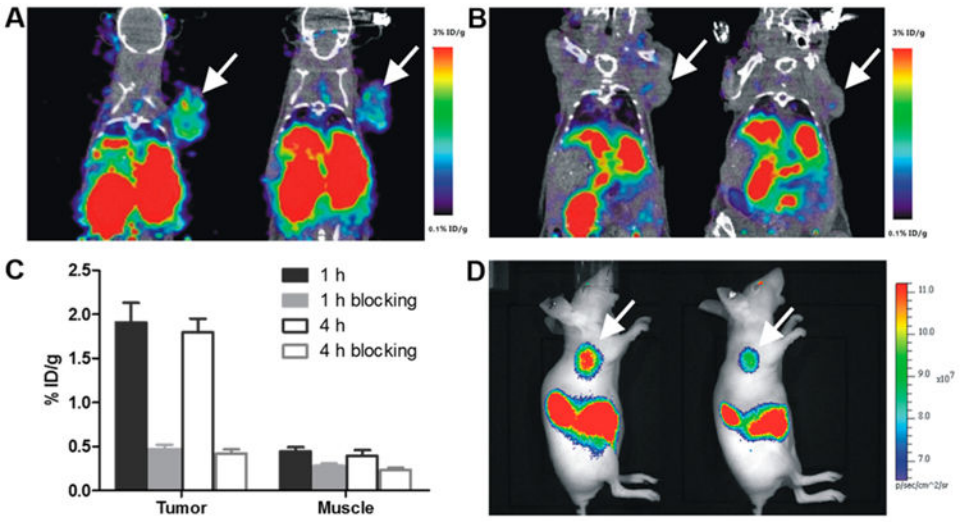

Figure 3.

PET/CT images of HT-29 tumor-bearing mice at 1 and 4 h postinjection of ^{64}Cu-DOTA-NT-Cy5.5 (A) without and (B) with a blocking dose of NT peptide. (C) The quantitative tumor and muscle uptakes derived from PET images. (D) *In vivo* fluorescent images of HT-29 tumor-bearing mice.

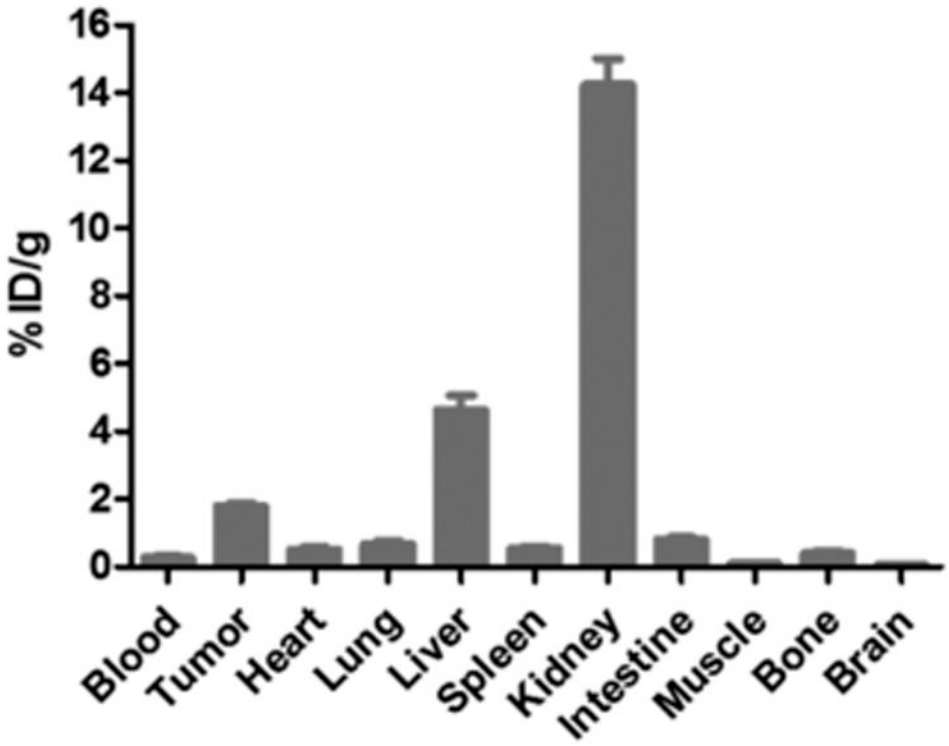

Figure 4.
Biodistribution of ^{64}Cu-DOTA-NT-Cy5.5 in mice bearing HT-29 xenograft at 4 h p.i.

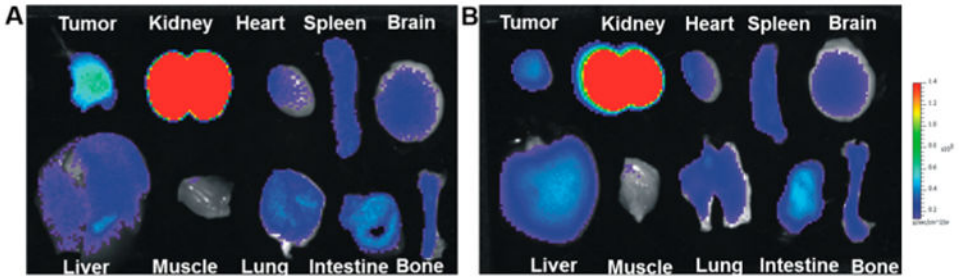

Figure 5.

Ex vivo fluorescent images of major organs harvested at 4 h p.i. of ^{64}Cu-DOTA-NT-Cy5.5 (A) without and (B) with coinjection of Cys-NT.

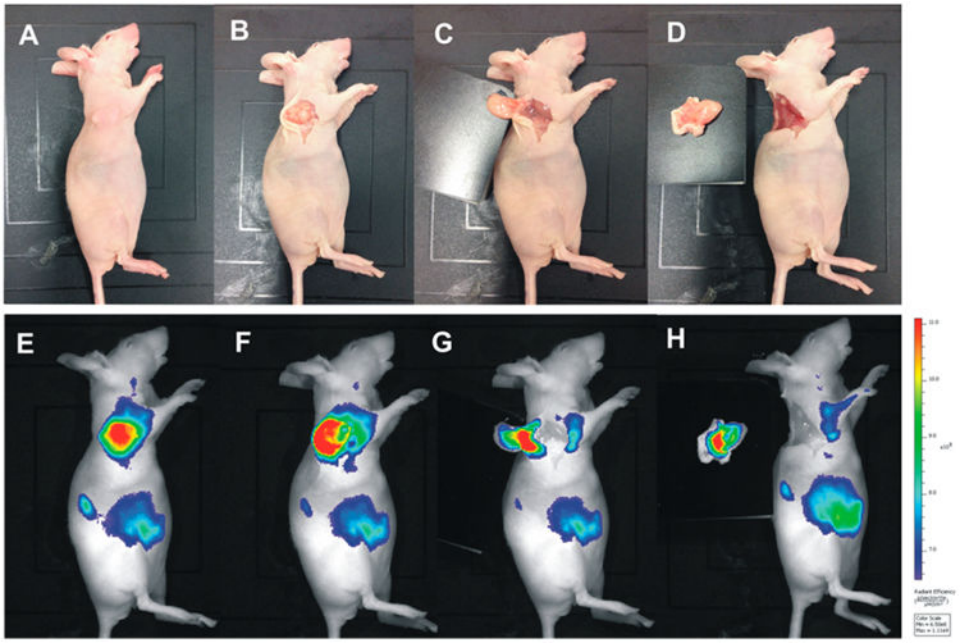

Figure 6.

Athymic female nude mouse bearing HT-29 tumor at 4 h postinjection of ^{64}Cu-DOTA-NT-Cy5.5. The tumor lesion was subsequently removed by fluorescent image-guided surgery. (A–D) Digital pictures of the mouse and the tumors during surgery. (E–H) Fluorescent images as a visual guide during surgery.

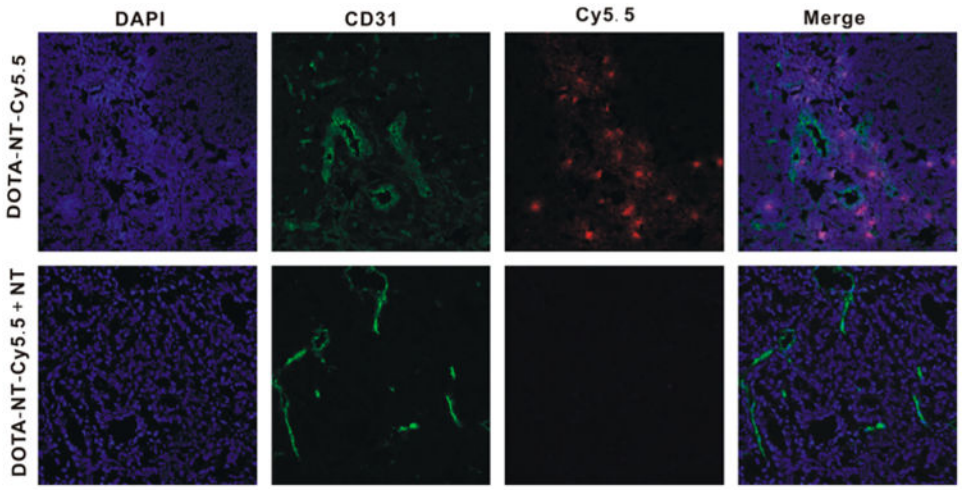

Figure 7.

In vivo functional targeting of the novel DOTA-NT-Cy5.5. Representative serial sections of HT-29 xenograft tumors stained with DAPI (blue), CD31 antibody (green), and DOTA-NT-Cy5.5 (red).

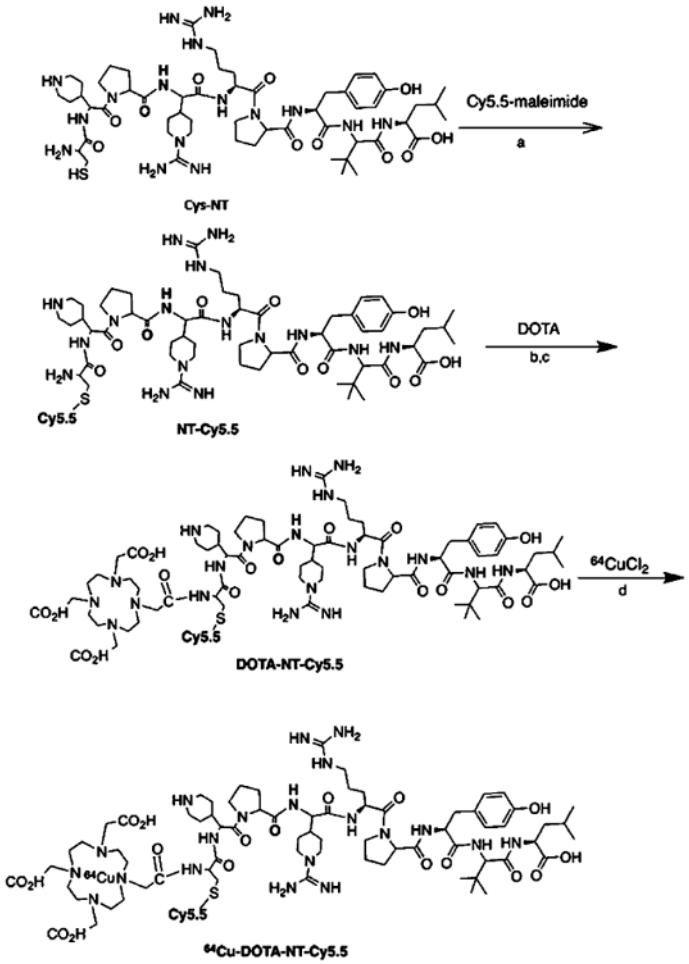

Scheme 1. Synthesis of ^{64}Cu-DOTA-NT-Cy5.5[a]

[a]Reagents and conditions: a. pH 7.5, 30 min RT. b. EDC/SNHS, pH = 5.5. c. borate buffer (pH 8.5), 30 min RT. d. NH_4OAc (pH 5.5), 37 °C, 60 min.